

OBSERVATION OF THE 1973 SOLAR ECLIPSE IN MAURITANIA

Takumi Mori* and Yasuhiro Ganeko*

*Received 21 October 1975***Abstract**

At the total solar eclipse on June 30, 1973, an observation of contact times was made at Atar, Mauritania, by means of cinematography of the flash spectra. The atmospheric transparency at the total phase was not so fair, but it might not act so seriously on the photometry of the continuum of the spectra, judging from the growth of the eclipse curves. Although resultant profiles of the moon agree generally with those of Watts' charts, a large discrepancy is found between $\Pi=280^\circ$ and 290° . It might be attributed to some defects of Watts' charts. Excluding these portions and counting out the data such that the reduced eclipse curves have abnormal shapes, the apparent relative position of the moon to the sun at that time is determined on the current ephemerides. Assuming $ET-TAI=32.^s0$, the observed position minus calculated one is found to be :

$$\Delta(L\kappa - L\sigma) = +0.^s39 \pm 0.^s02 \text{ (m.e.)},$$

$$\Delta(\beta\kappa - \beta\sigma) = +0.43 \pm 0.13 \text{ (")}.$$

1. Observation

The government of the Islamic Republic of Mauritania provided the Atar airport as the observation site. Atar lies on the southwest edge of the Sahara Desert. In this site the black sun was viewed at 60° in altitude and 80° from north to east.

The principle and the method of contact time observation adopted for this event are the same as those for the 1970 eclipse (T. Mori and Y. Kubo, 1971). Spectra of the extreme edge of the sun's disk are taken at the 2nd and 3rd phases by a 16 mm-movie camera with a precise timing device. Photometric measurements on a continuum region of the spectra are made along the moon's limb. From the time sequence of the photometric data, the eclipse curves are drawn against time for the contour points, which are situated with roughly equal interval on the moon's limb, and then the respective contact times are defined by reading the inflection points of the curves.

The equipment for the observation was identical with one used in 1970, with an exception that the objective lens of the camera was replaced from an achromat ($\phi=60\text{mm}$, $f=930\text{mm}$) to an apochromat ($\phi=80\text{mm}$, $f=1200\text{mm}$). The diameter of the moon's image at this time was 11.83mm and dispersion was 56A/mm at $\lambda=4615\text{A}$. Kodak plus X (ASA 80 in daylight) was adopted as the sensitive material.

* Astoronomical Division, Hydrographic Department

Time signals on WWV 10 MHz were received to keep the local clocks. These receptions were possible at this site only between 06^h30^m and 07^h00^m UT every day in this June. The geodetic position of the telescope was determined by means of the doppler observations of Navy Navigation Satellite System (NNSS).

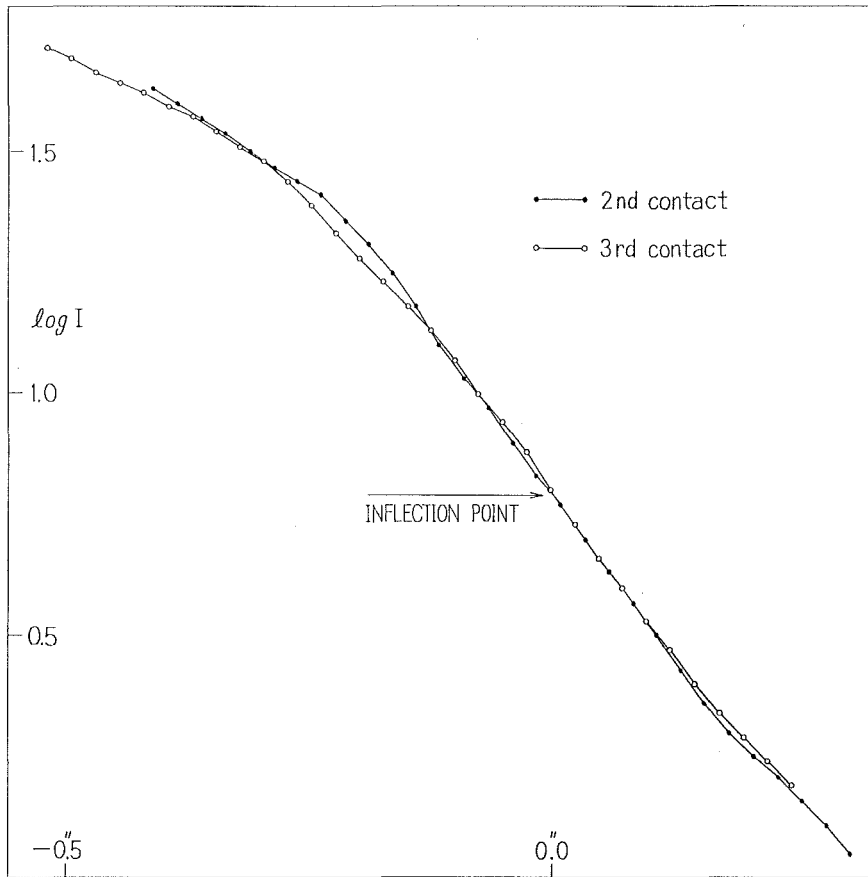
On June 30, the day of the eclipse, a hard sand storm was to blow in the afternoon. In the morning it was partially cloudy and temperature was abnormally high. At the total phase of the eclipse, there was thin cloud in the sky and a cloud of sand was drifting in the atmosphere. The latter brought about only one degree drop in atmospheric temperature at the totality, while 4°C-fall was recorded even on the seacoast in Mexico in 1970.

The flash spectra were photographed at a rate of 14.5 shot per second from 10^h43^m55^s to 10^h44^m40^s UT for the 2nd contact and from 10^h49^m55^s to 10^h50^m43^s UT for the 3rd contact. The exposure time was 0.^s021 per shot. For the calibration of photographic density against incidental intensity, photographs of Fraunhofer spectra were taken immediately after the eclipse. The performances of the equipment were satisfactory all through the observation.

2. Photometry

The development of the films was made by a private laboratory in Tokyo. The photographs are fairly good except for some kinds of astigmatism detected in the direction of dispersion. Photographic measurements were made on 80 frames each for the 2nd and 3rd contact. A slit of 200 μ width (corresponding to 0.^o23 in position angle along the moon's limb) swept 11A band width centered at 4615A and measured density at the contour points. The resultant eclipse curves are shown in Fig. 1. Both of them are means of 3 individual curves on the distinct contour points for the 2nd and 3rd contacts, respectively. The curve for the 3rd contact was suffered a little from abnormal atmospheric absorption without no serious effects. The definition of inflection points, on which the edge of the sun was defined as had been done for the 1970 eclipse, seems to be secured within an accuracy of 0.^o05 in the radius. The maximum gradient $d \log / dh = 2.7 / \text{sec of arc}$. This value agrees quite well with the result obtained for the 1970 eclipse.

Then, contact times of respective contour points on the moon's limb to the sun's edge defined above are determined through least squares fittings of photometric data. In the 1st and 2nd columns of Table 1 and 2, the raw observation data are given. The 1st column involves the linear measures x on the photomicrometer in an arbitrary dimension of length. Suffixes m , v and p denote that the points correspond to apparent mountain, valley and plateau on the moon's limb, respectively. The contact times t_c in UTC in the 2nd column are, of course, applied with the small corrections described in the 1970 eclipse report. Asterisk (*) in this column shows that the gradient of the eclipse curve at this point is smaller than 3/4 of the normal gradient and they are to be excluded from the further analysis. In the 3rd column, the Watts' angle Π_W corresponding to the points are given. They are established in-

Fig. 1 Eclipse Curve at $\lambda=46154$

ductively through comparison of the observation with predictions.

3. Position of the telescope

The geocentric position of the observation site was fixed by making use of NNSS. Doppler observations of 84 passes of 6 satellites were made by a JRC receiver. The geodetic coordinates deduced through the IAU 1964 parameters are as follows.

$$\varphi = 20^{\circ}30'17.''70N \pm 0.''14 \text{ (m. e.)},$$

$$\lambda = 346^{\circ}57'11.29E \pm 0.10 \text{ (")},$$

$$H = 278.0\text{m} \pm 2.9\text{m} \text{ (")}.$$

Astronomical observations for longitude and latitude were also made in 4 nights. The vertical deflection referring to the above system is:

$$\xi \equiv \varphi_a - \varphi_g = -0.''90 \pm 0.''20 \text{ (m. e.)},$$

$$\eta \equiv (\lambda_a - \lambda_g) \cos \varphi = -4.65 \pm 0.20 \text{ (")},$$

where sense of λ is positive to the east.

4. Local prediction

In the present reduction, the following ephemerides and the related quantities are adopted.

(i) Sun

The ecliptic coordinates of the sun in the AE are corrected to the IAU 1964 system and then converted into the equatorial coordinates shown bellow.

ET 0 ^h	α_{app}	δ_{app}
Jun. 30	6 ^h 35 ^m 7. ^s 778	+23°11'50."59
Jul. 1	6 39 16.270	+23 8 9.68

(ii) Moon

The AE is adopted.

(iii) Miscellaneous

$$ET - TAI = 32.^s0$$

$$TAI - UTC = 12.0$$

$$UT1 - UTC = + 0.23 \text{ (BIH, 1974)}$$

$$II - II_W = - 0.^o2 \text{ (assumed)}$$

$$\bar{r}_\odot = 15'59."63 \text{ (Auwers, 1891)}$$

$$k = 0.2725026$$

The precise predictions for this site are:

	2nd contact	3rd contact	description
t_0	10 ^h 44 ^m 12. ^s 27	10 ^h 50 ^m 19. ^s 09	contact time in UTC
p_0	259. ^o 91	113. ^o 38	contact angle
r_\odot	15'43."88	15'43."88	topocentric radius of the sun
v	0."3847/sec	0."3815/sec	apparent motion of the moon relative to the Sun
ϕ	96. ^o 46	96. ^o 88	
$r_\zeta - r_\odot$	73."26	73."47	

The topocentric places of the sun and the moon and their derivatives to ET at the 2nd contact are:

$$\alpha_\zeta = 6^h36^m54.^s189 \quad \dot{\alpha}_\zeta = +0.^s046/sec \quad \alpha_\odot = 6^h36^m59.^s420 \quad \dot{\alpha}_\odot = +0.^s003/sec$$

$$\delta_\zeta = +23^\circ10'1."73 \quad \dot{\delta}_\zeta = -0."10/sec \quad \delta_\odot = +23^\circ10'14."57 \quad \dot{\delta}_\odot = -0."00/sec$$

The topocentric libration of the moon at the totality is:

$$l = +1.^o54, \quad b = +0.^o05, \quad \text{and} \quad C = 2.^o17.$$

5. Reduction

The method of reduction is almost the same as that adopted for the 1970 eclipse, the details being not presented here.

The observation times are reduced to the heights h (in the 4th column of Tables 1 and 2) of the true limb from the circular moon, being at the predicted position, through the formula:

$$h = -(r_\zeta - r_\odot)_i \{1 + \cos(p - p_{0i})\} - v_i(t_c - t_{0i}) \cos(p - \phi_i) - (r_\zeta - r_\odot)_i^2 / 2r_\odot \cdot \sin^2(p - p_{0i})$$

$$(i=2, 3),$$

where $i=2$ and 3 stand for the 2nd the 3rd contacts, respectively.

In the 5th column of Tables 1 and 2, corresponding height h_W in Watts' charts are given. They have been interpolated by smoothing from the original values and deduced to those at the true distance.

In Fig. 2 and 3, two contours are plotted, respectively. The observed ones are linked by solid lines. The circle corresponds to the observation marked by asterisk in the 2nd column of the Tables. The Watts' profiles are shown by dotted lines. They are coincident mutually, but between $II_W=280^\circ$ and 290° at the 3rd contact, large discrepancies appear. Considering that any distinguished anomaly is not found on the eclipse curves in this region and those in the other region where the exposures were made at the same instances, this discrepancy seems to be due to a defect in the Watts' charts. Then, they are excluded in the present analysis and marked by asterisks (*) in the 5th column of the Tables and are also shown by circles in the Figs. 2 and 3.

The least squares method is applied to the following equation :

$$\cos p \cdot \Delta(\delta_\epsilon - \delta_\circ) + \sin p \cdot \Delta(\alpha_\epsilon - \alpha_\circ) \cos \delta_\circ + \Delta(r_\epsilon - r_\circ) + h_W - h = 0$$

The solution is :

$$\Delta(\delta_\epsilon - \delta_\circ) = +0.40 \pm 0.13 \text{ (m. e.)},$$

$$\Delta(\alpha_\epsilon - \alpha_\circ) \cos \delta_\circ = +0.42 \pm 0.02 \text{ (")},$$

$$\Delta(r_\epsilon - r_\circ) = -0.38 \pm 0.04 \text{ (")},$$

or, in the ecliptic coordinate :

$$\Delta(L_\epsilon - L_\circ) = +0.39 \pm 0.02 \text{ (m. e.)},$$

$$\Delta(\beta_\epsilon - \beta_\circ) = +0.43 \pm 0.13 \text{ (")}.$$

In the 6th columns of Table 1 and 2, residuals (v) for this solution are given. They show winding trends against position angle. It means that the observed/Watts' profiles are suffered portionally from systematic errors, and that, therefore, the formal errors calculated above are much smaller than true ones.

6. Concluding remarks

- (i) Observations like the present one are feasible only when the reduction analysis can be made with reference to a map of the moon's profiles. Considering, further, the composition procedure of the Watts' charts, there is no positive reason to claim that only a very limited part of the Watts' charts is incorrect. Therefore, it may be a fatal deficiency for the present solution to have excluded a part of observations due to its disagreement with the Watts' charts solely. When we consider a result of a similar comparison with the Weimer's profile, however, the Watts' charts seem to be particularly erroneous in the very part as long as the 1973 eclipse observation is concerned. There is no further explanation for this disagreement for the present.
- (ii) The principle of our eclipse observation utilizes a merit that the sun's semidiameter need not to be specifically defined, provided that the sun has a spherically symmetrical shape. However, in the reduction analysis of the present observation, the separation of the differences of the semidiameters and declinations was bad to solve the observation equations due to the facts that the sun appeared smaller while

TABLE 1. OBSERVATION DATA (2nd contact)

x	t_c	Π_W	h	h_W	v	x	t_c	Π_W	h	h_W	v
	$10^{\text{h}44^{\text{m}}}$		"	"	"		$10^{\text{h}44^{\text{m}}}$		"	"	"
19.7	8.97	87.30	+0.21	+0.14	-0.02	81.5	11.81	77.23	+0.16	+0.09	+0.04
21.2 p	9.20	87.04	+0.18	+0.14	+0.01	83.0	11.69	77.00	+0.20	+0.22	+0.12
23.0	9.40	86.73	+0.17	+0.04	-0.08	84.5	11.47	76.77	+0.28	+0.23	+0.06
24.5 p	9.63	86.47	+0.13	+0.09	+0.01	86.1 m	11.35	76.52	+0.31	+0.32	+0.12
26.0	9.93	86.21	+0.07	+0.06	+0.04	87.5	11.57	76.28	+0.22	+0.17	+0.06
27.4 v	10.14	85.97	+0.04	+0.03	+0.04	89.0	12.03	76.02	+0.04	-0.03	+0.04
29.0	9.79	85.70	+0.22	+0.16	0.00	90.5	12.39	75.76	-0.10	-0.17	+0.05
30.5	9.33	85.44	+0.44	+0.50	+0.12	92.0	12.67	75.50	-0.22	-0.35	-0.01
32.0	8.89	85.19	+0.65	+0.80	+0.21	93.5	13.04	75.28	-0.36	-0.46	+0.02
33.4 m	8.65	84.94	+0.78	+0.87	+0.15	95.0	13.50	75.05	-0.55	-0.51	+0.16
35.0	8.93	84.67	+0.72	+0.75	+0.09	96.5	13.79	74.83	-0.67	-0.59	+0.20
36.5	9.49	84.41	+0.55	+0.52	+0.03	97.8 v	13.95	74.64	-0.74	-0.68	+0.18
38.0	10.19	84.15	+0.32	+0.40	+0.15	99.6	13.55	74.37	-0.62	-0.79	-0.05
39.7 m	10.50	83.86	+0.25	+0.25	+0.07	101.0	13.30	74.16	-0.54	-0.89	-0.23
41.0	10.85	83.64	+0.15	+0.12	+0.04	102.5	13.18	73.94	-0.52	-0.87	-0.23
42.4 v	11.18	83.40	+0.05	+0.06	+0.08	104.0	13.15	73.71	-0.53	-0.82	-0.16
44.0	10.59	83.15	+0.31	+0.19	-0.05	105.5	13.19	73.49	-0.57	-0.89	-0.19
45.5	10.19	82.91	+0.49	+0.34	-0.08	106.9 v	13.35	73.28	-0.65	-0.84	-0.06
47.3 m	9.95	82.63	+0.61	+0.48	-0.05	108.5	13.14	73.04	-0.60	-0.77	-0.04
48.6 v	9.98	82.42	+0.62	+0.53	-0.01	110.0 m	12.93	72.82	-0.55	-0.79	-0.11
49.6 m	9.97	82.27	+0.64	+0.53	-0.03	111.5	13.17	72.59	-0.67	-0.89	-0.09
51.0	10.15	82.05	+0.59	+0.47	-0.04	112.7 v	13.41	72.42	-0.77	-0.99	-0.09
52.4	10.55	81.83	+0.46	+0.37	-0.01	114.5	13.12	72.15	-0.71	-0.87	-0.03
53.6 v	10.89	81.64	+0.35	+0.29	+0.02	116.0	12.78	71.92	-0.62	-0.73	+0.03
56.0 m	10.51	81.26	+0.53	+0.34	-0.11	117.5	12.24*	71.70	-0.46	-0.53	
57.0	10.55	81.10	+0.52	+0.38	-0.05	119.0	11.74*	71.46	-0.32	-0.16	
58.3	10.64	80.90	+0.50	+0.35	-0.06	120.6	11.37*	71.20	-0.23	-0.03	
59.7	10.82	80.68	+0.45	+0.27	-0.09	122.0	11.02*	71.97	+0.02	-0.77	
61.0	11.48	80.47	+0.22	+0.17	+0.04	123.5	10.78*	70.73	-0.10	+0.27	
62.4	11.87	80.25	+0.08	+0.05	+0.06	125.0	10.40*	70.49	-0.01	+0.19	
64.0	12.08	80.00	+0.02	-0.12	-0.05	126.5	10.05*	70.25	+0.07	+0.23	
65.5	12.24	79.76	-0.03	-0.21	-0.09	128.0	9.79*	70.00	+0.11	+0.38	
67.0	12.56	79.52	-0.14	-0.31	-0.08	129.5 m	9.61*	69.76	+0.13	+0.29	
68.4	12.83	79.30	-0.23	-0.36	-0.03	131.5 v	9.64*	69.44	+0.05	+0.11	
70.3 v	12.95	78.99	-0.27	-0.41	-0.04	132.3	9.55*	69.31	+0.05	+0.03	
72.0	12.90	78.72	-0.24	-0.35	-0.01	133.6 m	9.47*	69.10	+0.04	-0.06	
74.0	12.54	78.40	-0.10	-0.21	-0.01	135.0	9.78	68.87	-0.12	-0.27	0.00
75.6 m	12.29	78.15	-0.01	-0.25	-0.14	136.6 v	10.05	68.52	-0.30	-0.44	+0.01
77.4 v	12.37	77.87	-0.04	-0.31	-0.17	138.0	9.82	68.39	-0.25	-0.38	+0.02
78.5	12.25	77.70	+0.01	-0.30	-0.20	139.5	9.37	68.15	-0.15	-0.08	+0.22
80.0	12.00	77.47	+0.10	-0.19	-0.18	141.0	9.01*	67.90	-0.09	+0.06	

TABLE 2. OBSERVATION DATA (3rd contact)

x	t_c	H_W	h	h_W	v	x	t_c	H_W	h	h_W	v
9.0	10 ^h 50 ^m 19.07	279.80	-1.63	-0.88*		71.7	10 ^h 50 ^m 16.90	289.92	-0.83	-0.36*	"
10.7	18.76	280.07	-1.67	-1.22*		73.2m	17.19	290.16	-0.72	-0.43*	
12.0	18.58	780.28	-1.68	-1.40*		74.8 v	17.08	290.42	-0.75	-0.40*	
13.5	18.35	280.52	-1.71	-1.57*		76.0	17.18	290.62	-0.71	-0.35*	
15.0	18.11	280.76	-1.74	-1.77*		77.5	17.53	290.86	-0.58	-0.17*	
16.5	17.92	281.01	-1.74	-1.86*		79.0 v	17.75	291.10	-0.49	+0.00	-0.12
18.0	17.73	281.25	-1.76	-1.84*		80.5m	17.98	291.34	-0.41	+0.13	-0.07
19.2	17.48	281.44	-1.81	-1.91*		82.0	18.24	291.59	-0.31	+0.19	-0.11
21.0	17.37	281.73	-1.78	-1.97*		83.5	18.31	291.83	-0.29	+0.22	-0.09
22.3 v	17.26	281.94	-1.77	-2.03*		85.0	18.31	292.07	-0.29	+0.22	-0.09
23.5 v	17.31	282.14	-1.71	-2.04*		86.5	18.49	292.31	-0.23	+0.32	-0.05
25.1 v	17.20	282.40	-1.69	-2.12*		88.0	18.71	292.56	-0.15	+0.36	-0.09
26.5	17.55	282.62	-1.51	-2.04*		89.5	19.02	292.80	-0.05	+0.45	-0.09
28.2	17.98	282.90	-1.29	-1.91*		91.0	19.25	293.04	+0.03	+0.61	-0.01
30.2m	18.24	283.22	-1.13	-1.64*		92.9m	19.48	293.35	+0.10	+0.66	-0.03
31.6 v	18.21	283.44	-1.10	-1.41*		94.8 v	19.31	393.59	+0.02	+0.68	+0.07
32.7m	18.24	283.62	-1.05	-1.30*		96.3	19.50	293.90	+0.07	+0.67	+0.02
33.8	18.09	283.80	-1.07	-1.11*		98.0	19.76	294.18	+0.15	+0.73	0.00
35.0	17.88	283.99	-1.12	-1.00*		99.8m	19.99	294.48	+0.21	+0.84	+0.05
36.3 v	17.78	284.20	-1.12	-0.94*		101.2	19.80	294.70	+0.12	+0.80	+0.10
37.5	17.83	284.40	-1.07	-0.90*		102.6 v	19.68	294.93	+0.06	+0.65	+0.02
38.8m	17.91	284.61	-1.00	-0.85*		104.2	19.83	295.19	+0.09	+0.60	-0.06
40.4m	18.11	284.87	-0.88	-0.75*		105.8	20.08	295.46	+0.16	+0.68	-0.05
42.3m	18.33	285.17	-0.75	-0.49*		107.3m	20.15	295.70	+0.16	+0.68	-0.05
43.6 v	18.30	285.38	-0.73	-0.28*		109.0	20.02	295.93	+0.08	+0.55	-0.09
45.6m	18.55	285.71	-0.59	-0.12*		111.0	19.59	296.20	-0.10	+0.37	-0.09
47.0	18.28	285.93	-0.67	+0.02*		112.5 v	19.49	296.40	-0.16	+0.31	-0.09
48.5	17.71	286.17	-0.85	+0.20*		113.8	19.71	296.62	-0.11	+0.37	-0.08
50.0 v	17.45	286.42	-0.91	+0.23*		115.3	20.34*	296.87	+0.08	+0.58	
51.2	17.64	286.61	-0.82	-0.19*		117.0	20.82*	297.16	+0.21	+0.75	
52.4	17.73	286.80	-0.76	+0.18*		118.5m	21.08*	297.41	+0.27	+0.88	
53.6m	17.92	287.00	-0.67	+0.20*		119.6	21.00*	297.59	+0.21	+0.85	
55.3 v	17.79	287.27	-0.69	+0.14*		120.8 v	20.88*	297.79	+0.14	+0.81	
56.5m	17.79	287.47	-0.67	+0.10*		122.0	21.01*	198.00	+0.15	+0.78	
57.4 v	17.77	287.61	-0.67	+0.09*		123.1m	21.18*	298.18	+0.18	+0.81	
58.5m	17.80	287.79	-0.64	+0.10*		124.2	21.07*	298.36	+0.11	+0.75	
60.3 v	17.70	288.08	-0.65	+0.10*		125.6 v	20.97	298.60	+0.03	+0.68	+0.11
61.8m	17.86	288.32	-0.57	+0.06*		127.0	21.11*	298.83	+0.04	+0.67	
63.0	17.60	288.52	-0.65	+0.00*		128.3m	21.24*	299.05	+0.05	+0.56	
64.5	17.26	288.76	-0.76	-0.07*		130.5 v	20.94	299.41	-0.13	+0.51	+0.11
65.8 v	17.15	288.97	-0.79	-0.15*		131.7m	21.02	299.60	-0.14	+0.47	+0.08
67.2m	17.23	289.19	-0.75	-0.33*		133.8 v	20.69	299.94	-0.32	+0.33	+0.12
68.2	17.07	289.36	-0.80	-0.34*		135.0	20.95	300.13	-0.27	+0.31	+0.06
69.5	16.81	289.57	-0.88	-0.26*		136.5	21.26*	300.37	-0.22	+0.29	
70.4 v	16.74	289.71	-0.90	-0.29*		138.2m	21.40*	300.65	-0.23	+0.20	

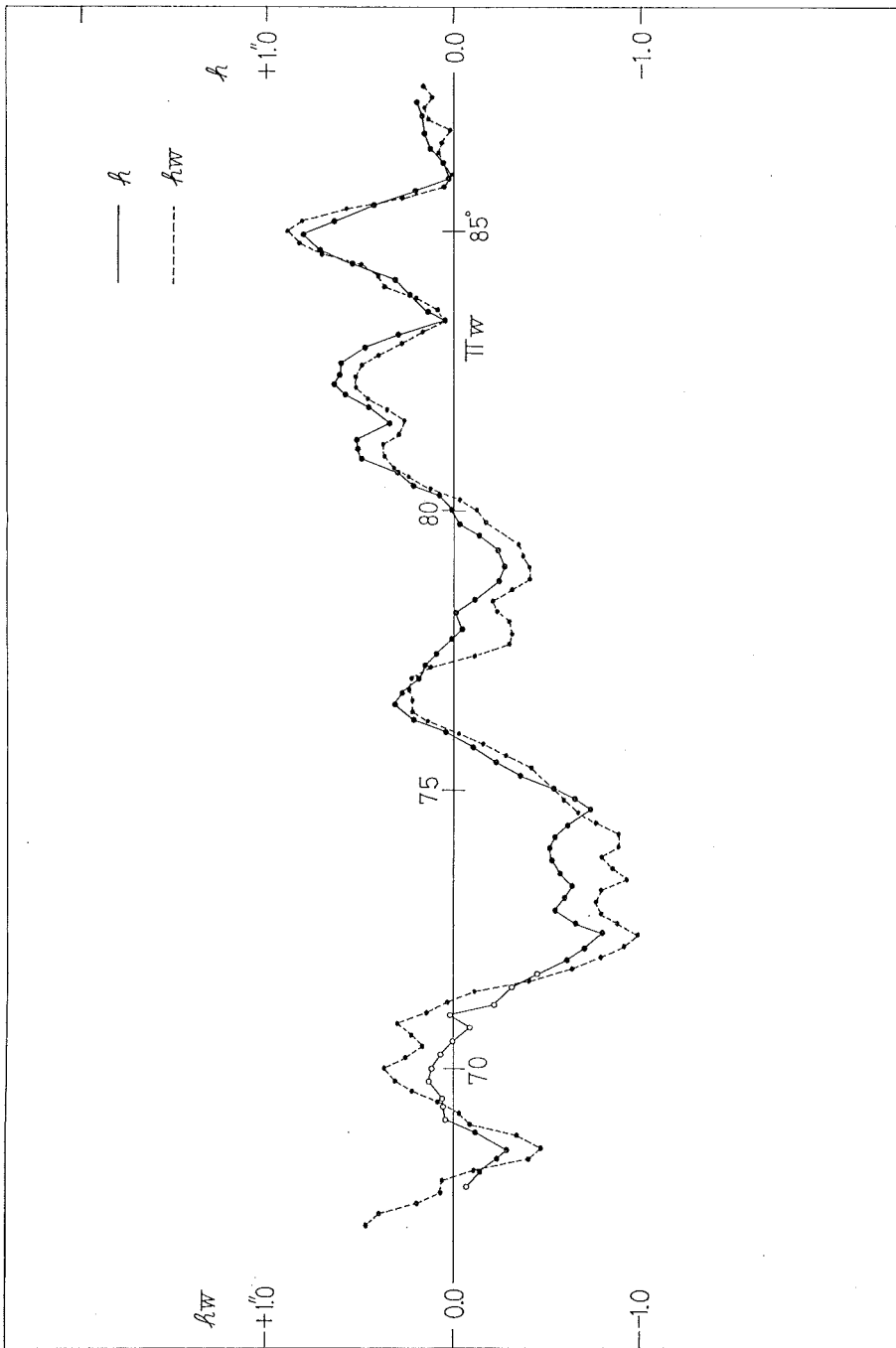


Fig. 2 Contour at the 2nd contact

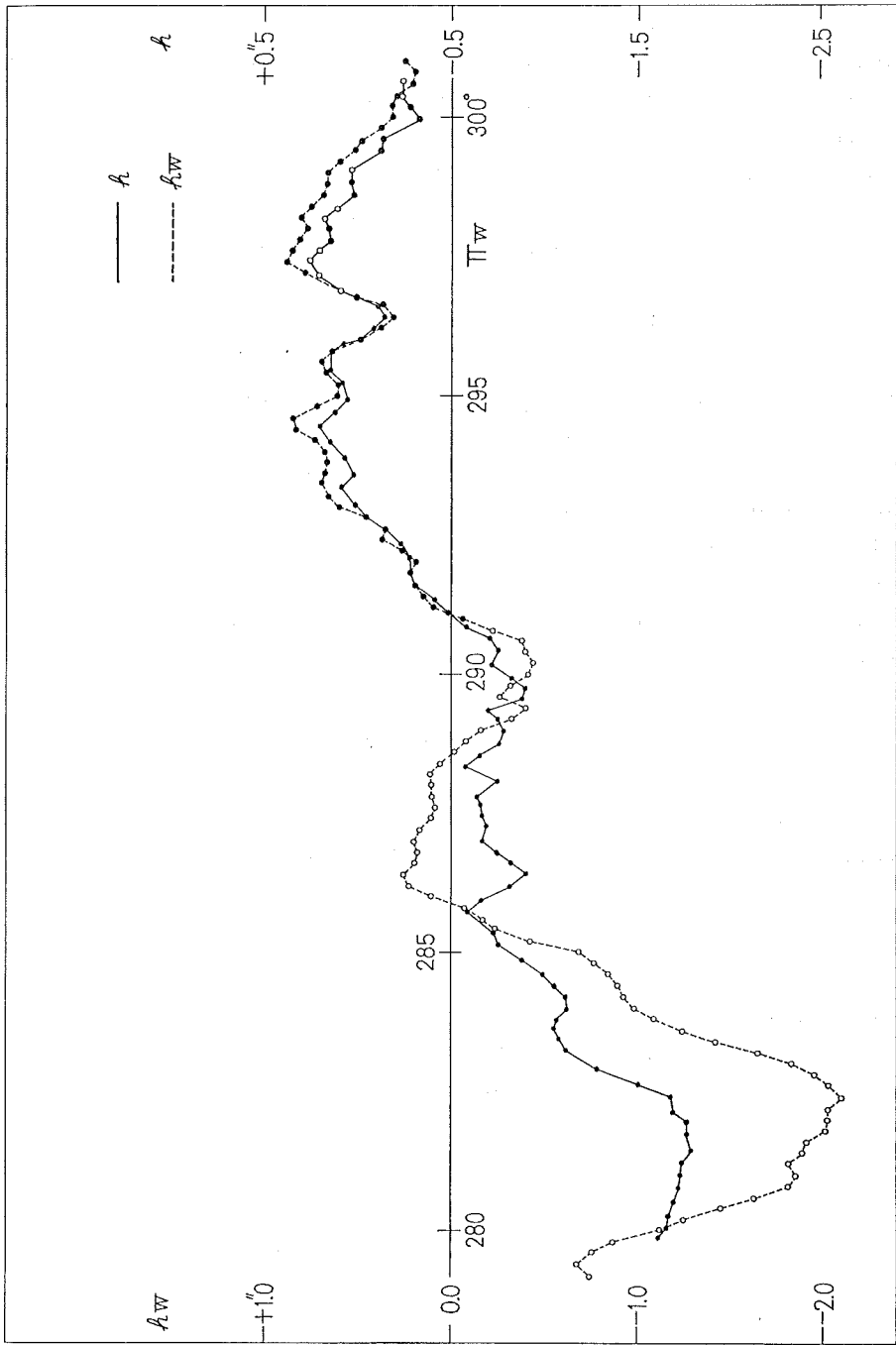


Fig. 3 Contour at the 3rd contact

the moon larger in the present event and that a part of the Watts' charts was abandoned. Hence, the differences of the semidiameters and the declinations have not been determined with good precisions.

Albeit, it may be said that, as far as we define the sun's semidiameter by means of the inflection point on the eclipse curves, such semidiameters agree well with each other within the error of photometry, i. e. within $\pm 0.''05$ for the present case.

Since we obtained a value $\Delta(r_{\epsilon} - r_{\odot}) = -0.''32 \pm 0.''02$ for the 1970 eclipse, the solution $-0.''38$ for the present case seems to be reasonable. If we impose, for trial, $-0.''32$ for the present data, the other solutions with an equal weight for each contact are

$$\Delta(\alpha_{\epsilon} - \alpha_{\odot}) \cos \delta_{\odot} = 0.''39 \pm 0.''01 \text{ (m. e.)},$$

$$\Delta(\delta_{\epsilon} - \delta_{\odot}) = 0.23 \pm 0.03 \text{ (")}.$$

Hence, we may consider that the solutions obtained in the preceding section have been well fixed somewhere around the ranges of the formal errors.

(iii) Final quality of reduction analysis of the present observation is entirely dependent on the quality of contour map as well as on that of the ephemerides. The contact times of each contour point on the moon's limb and the sun's edge, without ambiguity of the definition of the sun's edge, were determined quite accurately. The data presented in this paper will continue to be valuable and to produce good results depending on the improvement of accuracy of the contour of the moon's limb.

Acknowledgement

The authors wish to thank to the members of the expeditions from the Tokyo Astronomical Observatory, the Kwasan Observatory and the International Latitude Observatory of Mizusawa for helping the observation in Mauritania.

References

- BIH, 1974, Annual Report for 1973, Paris.
 Mori, T. and Kubo, Y., 1971, Report of Hydrographic Researches, 7, 39.
 Mori, T. and Kubo, Y., 1975, *ibid.* 10, in this issue.
 Watts, C.B., 1963, Astr. Pap. Amer. Eph. 17.
 Weimer, Th., 1952, Atlas de Profils Lunaires, Paris.